Neuron
Article

# Synaptic Accumulation of PSD-95 and Synaptic Function Regulated by Phosphorylation of Serine-295 of PSD-95

Myung Jong Kim,[1] Kensuke Futai,[1] Jihoon Jo,[2] Yasunori Hayashi,[1] Kwangwook Cho,[2] and Morgan Sheng[1,*]
[1]The Picower Institute for Learning and Memory, RIKEN-MIT Neuroscience Research Center, Howard Hughes Medical Institute, Massachusetts Institute of Technology, Cambridge, MA 02139, USA
[2]Henry Wellcome Laboratories for Integrative Neuroscience and Endocrinology, MRC Centre for Synaptic Plasticity, Faculty of Medicine and Dentistry, University of Bristol, Bristol BS1 3NY, UK
*Correspondence: msheng@mit.edu
DOI 10.1016/j.neuron.2007.09.007

## SUMMARY

**The scaffold protein PSD-95 promotes the maturation and strengthening of excitatory synapses, functions that require proper localization of PSD-95 in the postsynaptic density (PSD). Here we report that phosphorylation of ser-295 enhances the synaptic accumulation of PSD-95 and the ability of PSD-95 to recruit surface AMPA receptors and potentiate excitatory postsynaptic currents. We present evidence that a Rac1-JNK1 signaling pathway mediates ser-295 phosphorylation and regulates synaptic content of PSD-95. Ser-295 phosphorylation is suppressed by chronic elevation, and increased by chronic silencing, of synaptic activity. Rapid dephosphorylation of ser-295 occurs in response to NMDA treatment that causes chemical long-term depression (LTD). Overexpression of a phosphomimicking mutant (S295D) of PSD-95 inhibited NMDA-induced AMPA receptor internalization and blocked the induction of LTD. The data suggest that synaptic strength can be regulated by phosphorylation-dephosphorylation of ser-295 of PSD-95 and that synaptic depression requires the dephosphorylation of ser-295.**

## INTRODUCTION

PSD-95 is an important scaffold protein abundantly enriched in the PSD of excitatory synapses (Cheng et al., 2006; Kim and Sheng, 2004). PSD-95 contains three PDZ domains, an SH3 domain, and a guanylate kinase-like domain. The PDZ domains in particular mediate a wealth of interactions with intracellular signaling molecules and cell-surface adhesion molecules, ion channels, and receptors, including NMDA receptors (Kim and Sheng, 2004; Scannevin and Huganir, 2000).

PSD-95 promotes synapse maturation and exerts a major influence on synaptic strength and plasticity (El-Husseini et al., 2000; Elias et al., 2006). Overexpression of PSD-95 strongly potentiates AMPAR-mediated excitatory postsynaptic currents (EPSCs) (Beique and Andrade, 2003; Ehrlich and Malinow, 2004; El-Husseini et al., 2000; Elias et al., 2006; Futai et al., 2007; Nakagawa et al., 2004; Stein et al., 2003). Synaptic potentiation induced by the overexpression of PSD-95 shares some features with long-term potentiation (LTP), in that it converts silent synapses into functional synapses, drives GluR1 into synapses, and occludes LTP (Beique and Andrade, 2003; Ehrlich and Malinow, 2004; Stein et al., 2003). However, it is uncertain if LTP actually results from activity-induced recruitment of PSD-95 to synapses.

The synaptic targeting of PSD-95 depends on several domains within the protein (Craven et al., 1999). Palmitoylation of two cysteine residues in its N-terminal region is important for synaptic localization of PSD-95 and for synaptic potentiation by PSD-95 (Craven et al., 1999; El-Husseini et al., 2002). The level of PSD-95 palmitoylation is regulated by synaptic activity, and inhibition of palmitoylation is associated with loss of PSD-95 from synapses (El-Husseini et al., 2002). Because synaptic localization is essential for PSD-95's potent ability to promote synaptic strength, any molecular mechanism that affects the synaptic targeting or synaptic stability of PSD-95 could play an important role in the control of postsynaptic maturation and synaptic transmission.

Compared with palmitoylation (El-Husseini et al., 2002) and ubiquitination (Colledge et al., 2003) (but see Bingol and Schuman, 2004), surprisingly little is known about the regulation of PSD-95 by phosphorylation. Recent proteomic studies of phosphorylated proteins of the PSD fraction revealed that PSD-95 is phosphorylated on serine-295 (Jaffe et al., 2004; Trinidad et al., 2006), a residue lying between PDZ2 and PDZ3 of PSD-95. Here, we investigated the functional significance and molecular regulation of this phosphorylation. The phosphorylation of ser-295, which is bidirectionally modulated by synaptic activity in neurons, promotes the synaptic accumulation of PSD-95 and enhances synaptic potentiation by PSD-95. We

present evidence that ser-295 phosphorylation is mediated by Jun N-terminal kinase1 (JNK1) and dependent on Rac1, and that dephosphorylation of ser-295 is important for inducible AMPA receptor internalization and LTD. These results reveal a role for phosphorylation-dephosphorylation of a specific residue of PSD-95 in the control of synaptic function.

## RESULTS

### Phosphorylation of Ser-295 Promotes Synaptic Accumulation of PSD-95

PSD-95 is phosphorylated in the brain on ser-295, which lies in the sequence RRYSPVAK (Jaffe et al., 2004; Trinidad et al., 2006). We presume that this site is phosphorylated by a proline-directed kinase, such as a MAP kinase or CDK5.

To investigate the functional significance of PSD-95 ser-295 phosphorylation, we made mutants S295D-PSD-95 (to mimic ser-295 phosphorylation) and S295A-PSD-95 (to prevent ser-295 phosphorylation) and examined their subcellular localization in cultured hippocampal neurons. The level of protein expression of these mutant constructs was statistically the same as wild-type PSD-95 when transfected in neurons (Figure S1) and in heterologous cells (data not shown). Wild-type PSD-95 and S295D-PSD-95 showed a punctate pattern of staining along dendrites of transfected neurons, with a high degree of colocalization with surface GluR1 clusters and bassoon clusters (Figures 1A–1C). In contrast, the S295A-PSD-95 mutant showed considerable diffuse staining in the dendritic shaft in addition to high expression in spines (Figures 1A–1C). Thus, the S295A mutant concentrates at synapses less efficiently than wild-type or phosphomimic mutant of PSD-95.

The synaptic targeting of PSD-95 is essential for its ability to promote the surface expression of GluR1 AMPA receptors and to enhance the intensity of bassoon staining in presynaptic terminals that contact the transfected neuron (El-Husseini et al., 2000). By immunostaining, we found that S295D-PSD-95 and wild-type PSD-95 increased surface GluR1 levels by ~63% and by ~49%, compared to untransfected neurons (Figures 1B and 1D). The S295A-PSD-95 mutant, however, failed to enhance surface GluR1 immunoreactivity significantly (104.3% ± 11.4%; Figures 1B and 1D). Similarly, the intensity of bassoon immunostaining was significantly increased on neurons overexpressing S295D- or wild-type PSD-95, but not S295A-PSD-95 (Figures 1C and 1D). Thus, a single phosphorylatable residue (ser-295) influences synaptic abundance of PSD-95 and the ability of PSD-95 to recruit surface AMPA receptors and induce presynaptic accumulation of bassoon.

### Ser-295 Phosphorylation of PSD-95 Influences Synaptic Potentiation

We next compared the effect of overexpression of wild-type PSD-95, S295D-PSD-95, and S295A-PSD-95 on excitatory synaptic transmission in CA1 pyramidal neurons in hippocampal slice cultures (Figure 2). Simultaneous recording of EPSCs was performed from neighboring untransfected CA1 neurons and transfected CA1 pyramidal neurons that were identified by cotransfected GFP. Wild-type PSD-95 strongly enhanced AMPA-EPSCs (5.77 ± 0.89-fold relative to untransfected cells), as previously reported (Ehrlich and Malinow, 2004; Futai et al., 2007; Nakagawa et al., 2004; Schnell et al., 2002; Stein et al., 2003). Overexpression of the phosphomimicking mutant S295D-PSD-95 also caused a large increase in AMPA-EPSC (7.59 ± 1.51-fold), but the nonphosphorylatable S295A-PSD-95 was significantly less potentiating than wild-type (3.18 ± 0.57-fold) (Figures 2C and 2D). Overexpression of wild-type PSD-95 also significantly enhanced NMDA-EPSCs (1.88 ± 0.26-fold), similar to S295D-PSD-95 (1.80 ± 0.27) (Figures 2A, 2B, and 2D), though these effects were much smaller in degree than those on AMPA-EPSCs. NMDA-EPSCs were not significantly changed by S295A-PSD-95 (Figures 2C and 2D). Futai et al. also found a significant enhancement of NMDA-EPSC by PSD-95 overexpression (Futai et al., 2007).

### Phosphorylation of PSD-95 Ser-295 Regulated by Activity and by JNK

To study ser-295 phosphorylation of PSD-95 more directly, we generated phosphospecific antibodies (named "pS-295") against a phosphopeptide corresponding to this site [CSPRRY(pS)PVAKD]. On dot blots, the affinity-purified pS-295 antibody recognized the phosphopeptide [CSPRRY(pS)PVAKD] with good sensitivity, but showed no reactivity against the equivalent nonphosphorylated peptide (CSPRRYSPVAKD) (Figure S2A).

In immunoblots of hippocampal neuron cultures (DIV25–28), the pS-295 antibody recognized a major band of ~95 kDa (Figure S2B), consistent with a basal level of phosphorylation of PSD-95 on ser-295. Treatment of the neuron cultures with okadaic acid, an inhibitor of protein phosphatases PP1 and PP2A (100 nM, 2 hr) increased the intensity of this pS-295 band. Treatment of the membrane with calf intestine alkaline phosphatase abolished the pS-295 signal, without affecting the bands detected by antibody against total PSD-95 (Figure S2B). pS-295 antibody recognized a strong set of bands in COS-7 cells transfected with wild-type PSD-95, but not S295A-PSD-95 (Figure S2C). These data demonstrate that the pS-295 antibody specifically recognizes PSD-95 phosphorylated on ser-295 and that phosphorylation of ser-295 of PSD-95 occurs endogenously in neurons.

Which protein kinases might be responsible for the ser-295 phosphorylation of PSD-95 in neurons? We tested whether endogenous PSD-95 ser-295 phosphorylation could be altered by specific inhibitors of protein kinases in hippocampal neurons. Cultured hippocampal neurons (DIV24–28) were treated with KT5718 (5 μM, PKA inhibitor), KN-93 (10 μM, CaMKII inhibitor), PD98059 (25 μM, ERK pathway inhibitor), SB203580 (2.5 μM, p38 inhibitor), SP600125 (20 μM, JNK inhibitor), roscovitine (10 μM,

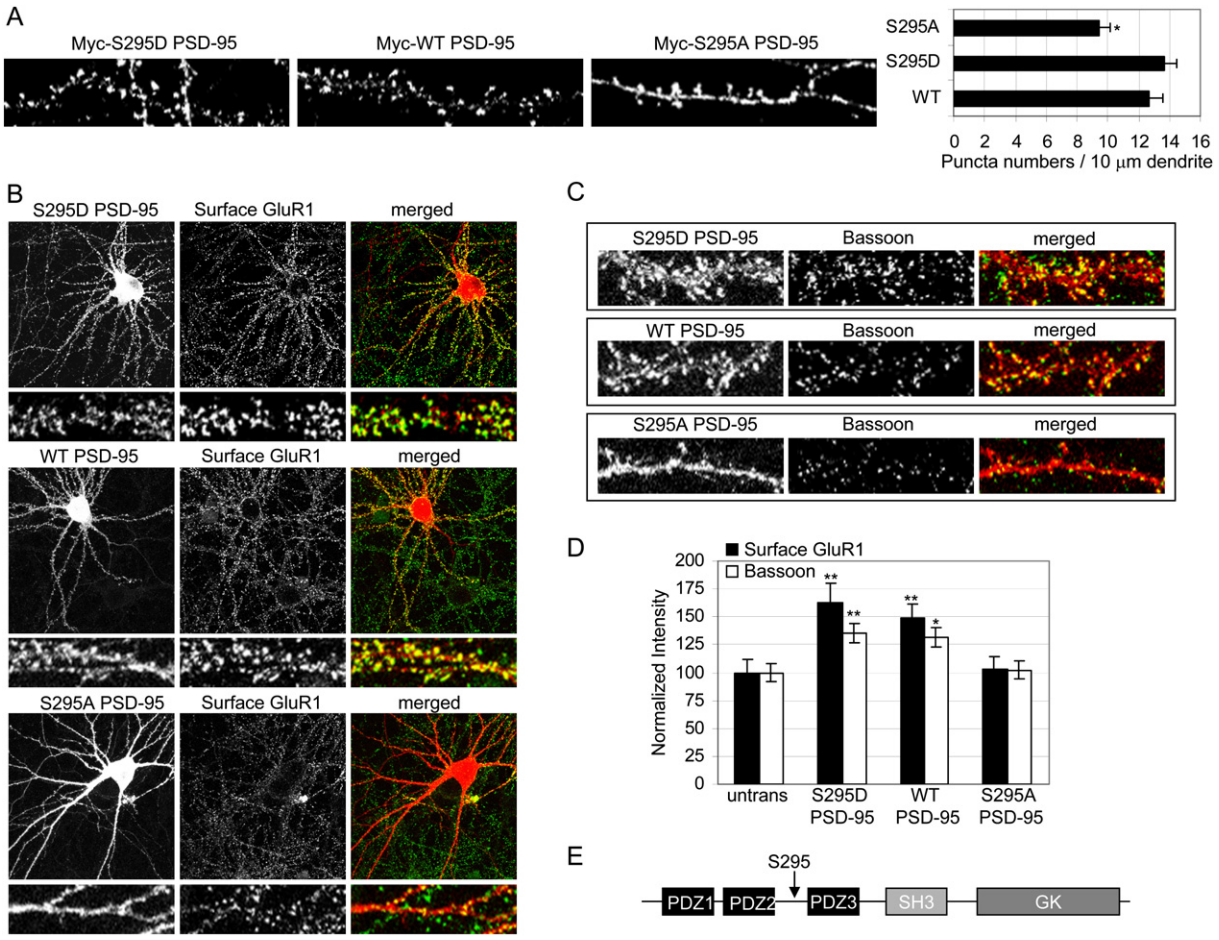


**Figure 1. Effects of PSD-95 Ser-295 Mutants on Synaptic Localization, Surface GluR1, and Bassoon**

(A) Localization of myc-tagged S295D-PSD-95, wild-type PSD-95, or S295A-PSD-95 in hippocampal neurons. Cultured hippocampal neurons were transfected at DIV14, and three days later were stained for myc. Bar graph shows mean ± SEM of number of myc puncta per 10 μm of dendrite. n = 16, 16, and 17 neurons from left to right. *$p < 0.05$, compared with WT-PSD-95.

(B) Effect of overexpression of S295D-PSD-95, wild-type PSD-95, or S295A-PSD-95 on surface GluR1 levels. Cultured hippocampal neurons were transfected at DIV14–15 and stained 3–4 days later for surface GluR1 (green) and PSD-95 (red). Individual channels are shown in grayscale.

(C) Effect of overexpression of S295D-PSD-95, wild-type PSD-95, or S295A-PSD-95 (red) on immunostaining of bassoon (green) on transfected neurons.

(D) Quantification of data from (B) and (C). Bar graph shows mean ± SEM of surface GluR1 and bassoon intensity, normalized to untransfected neurons. n = 15–20 neurons for each. *$p < 0.05$; **$p < 0.01$ compared with untransfected neurons or neurons transfected with S295A-PSD-95.

(E) Diagram of PSD-95, showing location of ser-295.

CDK5 inhibitor), or calphostin C (2 μM, PKC inhibitor) for 16 hr. Among these drugs, only the JNK inhibitor—SP600125—strongly reduced phospho-ser-295 levels relative to DMSO control (Figure 3A). The other MAP kinase pathway inhibitors (PD98059 and SB203580) at concentrations that block ERK and p38-signaling in neurons (Ehrlich and Malinow, 2004; Zhu et al., 2002) had little effect. KN-93 actually increased the pS-295 band. None of the pharmacological treatments for ~16 hr altered the total level of PSD-95 in cultured neurons (Figure 3A). A shorter 2 ht treatment with JNK inhibitor SP600125 also reduced phospho-S295 PSD-95 levels, whereas 2 hr treatment with other kinase inhibitors, including KN93, had no effect (Figure S3). These results suggest that JNK kinase activity is involved, directly or indirectly, in the phosphorylation of PSD-95 ser-295 in neurons.

Treatment of cultured hippocampal neurons (DIV25–28) with tetrodotoxin (TTX, 2 μM, 16 hr) increased phosphorylation of ser-295 (Figure 3A). In contrast, bicuculline (25 μM, 16 hr) suppressed ser-295 phosphorylation relative to DMSO control (Figure 3A). Similarly, in cultured hippocampal slices, phospho-ser-295 PSD-95 levels increased with TTX and decreased with bicuculline (Figure 3B). Thus, chronic changes in activity bidirectionally modulate ser-295 phosphorylation of PSD-95. We noted that the total PSD-95 band on western showed a subtle upward

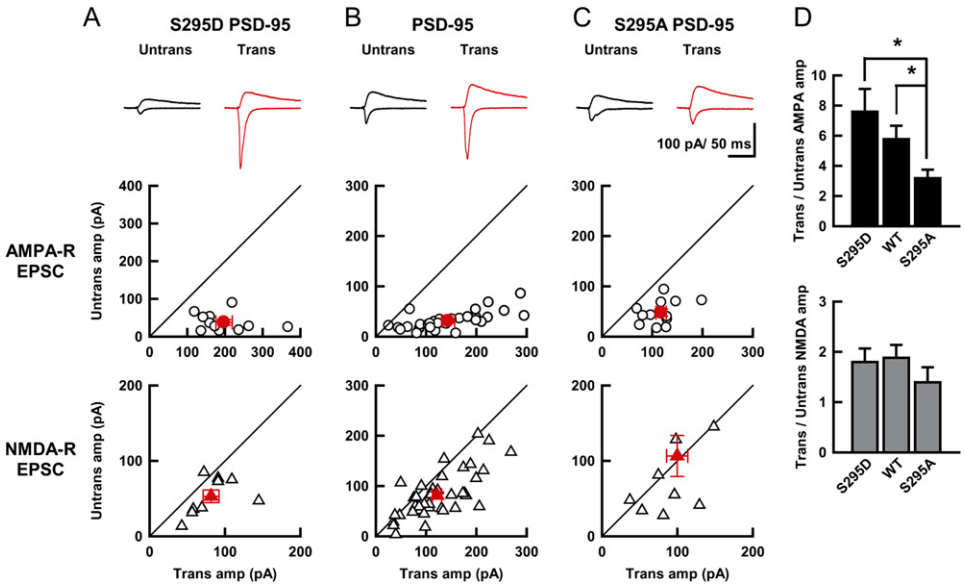


**Figure 2. Effect of Ser-295 Mutants of PSD-95 on Synaptic Transmission in Cultured Hippocampal Slices**

(A–C) (Top) Sample EPSC traces mediated by AMPA-R (downward) and NMDA-R (upward) from pairs of transfected (Trans) and neighboring untransfected (Untrans) cells. Stimulus artifacts were truncated. EPSC amplitudes (AMPA-R-EPSCs [middle] and NMDA-R-EPSCs [bottom]) were plotted for each pair of transfected and neighboring untransfected cells. Each open symbol represents a single pair of recordings. Mean ± SEM are shown by filled circles. (A) S295D-PSD-95 mutant. (B) Wild-type PSD-95. (C) S295A-PSD-95 mutant. PSD-95 and its variants enhanced AMPAR-EPSC amplitudes ($p < 0.00001$). In contrast, there were slight increases in the NMDAR-EPSC amplitude by the overexpression of PSD-95 ($p = 0.002$) and S295D-PSD-95 mutant ($p = 0.093$), but not S295A-PSD-95 mutant ($p = 0.623$).

(D) Summary of PSD-95 ser-295 mutant overexpression on AMPA-R-EPSCs (top) and NMDA-R-EPSCs (bottom). Each Bar graph represents average of ratios obtained from multiple pairs of transfected and untransfected neighboring neurons. Numbers of cell pairs were S295D (AMPA-R-EPSCs/NMDA-R-EPSCs: 11/9); wild-type (30/41); S295A (12/10). *$p < 0.05$, compared with neurons transfected with S295A-PSD-95.

mobility shift in cultures treated with TTX and KN-93, correlating with the increased phosphorylation on ser-295 (Figures 3A and 3B).

Even short-term exposure to bicuculline (25 μM; 5–20 min) reduced PSD-95 phospho-ser-295 levels in neurons, again without affecting total PSD-95 (Figure 3C). Treatment with TTX elevated PSD-95 phospho-ser-295 levels within tens of minutes, without affecting total PSD-95 (Figure 3C). These data indicate that ser-295 phosphorylation can be regulated rather quickly by synaptic activity.

Okadaic acid (100 nM, 2 hr) and calyculin A (20 nM, 2 hr), which act as inhibitors of protein phosphatases PP1 and PP2A, increased phosphorylation of ser-295; the PP2B inhibitor ascomycin (2–5 μM, 2 hr) had no effect (Figure 3D). Thus, PP1 and/or PP2A might be responsible for dephosphorylation of PSD-95 ser-295 in neurons.

Given that a JNK inhibitor suppressed phosphorylation of ser-295 in neurons, we next tested whether JNK can phosphorylate PSD-95 in vitro on this site. A purified bacterial hexahistidine-tagged fusion protein of approximately the N-terminal half of PSD-95 (amino acids 41–355) was used as substrate for in vitro kinase assays. The PSD-95 fusion protein was readily phosphorylated by activated recombinant human JNK1 (Upstate Biotech) on ser-295, as assayed by immunoblotting with pS-295 antibody (Figure 3E). Note that ser-295 phosphorylation is associated with a small upward mobility shift in the PSD-95 band on immunoblots (Figure 3E, asterisk). Moreover, JNK1 overexpression in COS-7 cells increased phosphorylation of cotransfected PSD-95 on ser-295, implying that JNK1 can phosphorylate PSD-95 on ser-295 in a cellular context as well as in vitro (Figure 3F).

## Postsynaptic Levels of PSD-95 and Phospho-Ser-295 Regulated by Activity and JNK

Our transfection experiments with ser-295 mutants of PSD-95 suggested that phosphorylation of this residue favors the postsynaptic accumulation of PSD-95 (Figure 1). If true, then the pool of PSD-95 that is phosphorylated on ser-295 should be more enriched in the PSD than total PSD-95. Indeed, compared with total PSD-95, the ser-295 phosphorylated form of PSD-95 was more highly enriched in PSD fractions of adult rat brain (Figure 4A; compare synaptosome versus PSDI and PSDII).

We used immunostaining with the pS-295 antibody to determine whether endogenous PSD-95 that is phosphorylated on ser-295 is specifically localized at synapses of cultured hippocampal neurons. As expected, pS-295 immunoreactivity colocalized with total PSD-95 in a punctate pattern along dendrites in basal conditions (Figure 4B; DMSO). To test whether PSD-95 synaptic targeting correlates with phosphorylation on ser-295, we modulated synaptic activity with TTX and bicuculline, which have opposite effects on phospho-ser-295 levels (see Figures 3A

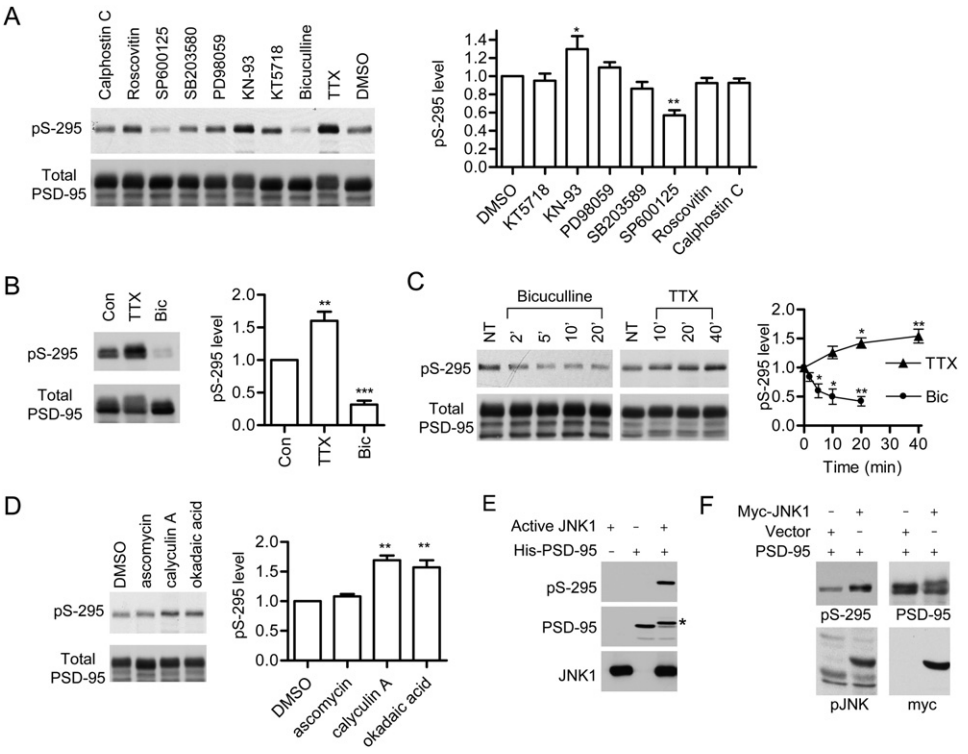


**Figure 3. Specificity of pS-295 Antibody, and Regulation of Phospho-Ser-295 PSD-95 Levels by JNK and by Activity**

(A) Effects of pharmacological kinase inhibitors and neuronal activity modulators on phospho-ser-295 levels of PSD-95. Cultured hippocampal neurons at DIV 25–28 were treated with DMSO, 2 μM TTX, 25 μM bicuculline, KT5718 (5 μM, PKA inhibitor), KN-93 (10 μM, CaMKII inhibitor), PD98059 (25 μM, ERK inhibitor), SB203580 (2.5 μM, p38 inhibitor), SP600125 (20 μM, JNK inhibitor), roscovitine (10 μM, CDK5 inhibitor), or calphostin C (2 μM, PKC inhibitor) for ~16 hr, and then immunoblotted with pS-295 antibody. After stripping, the blot was reprobed with mouse PSD-95 antibody. Graph shows pS-295 immunoblot intensity (divided by total PSD-95 intensity) normalized to DMSO control (mean ± SEM of five independent experiments). Statistical analysis was performed by one-way ANOVA, followed by the Dunnett's test. *$p < 0.01$; **$p < 0.01$ compared with DMSO control.

(B) Effect of bicuculline (25 μM) or TTX (2 μM) treatment for ~16 hr on phospho-ser-295-PSD-95 levels in organotypic slice cultures of rat hippocampus, measured by immunoblotting as in (A). Graph shows pS-295 level (divided by total PSD-95 level), normalized to DMSO control (n = 4). Statistical analysis was performed by one-way ANOVA, followed by the Dunnett's test. ***$p < 0.001$; **$p < 0.01$, compared to untreated control.

(C) Acute bidirectional modulation of phospho-ser-295-PSD-95 levels by bicuculline and TTX. Cultured hippocampal neurons (DIV25–28) were treated with bicuculline (25 μM) or TTX (2 μM) for the indicated time (min), and immunoblotted as in (A). Graphs show time course of pS-295 levels (divided by total PSD-95 level), normalized to untreated cells (n = 3). Statistical analysis was performed by one-way ANOVA, followed by the Dunnett's test. *$p < 0.05$; **$p < 0.01$, compared to untreated control.

(D) Effect of phosphatase inhibitors on phospho-ser-295 levels. Cultured hippocampal neurons at DIV25–28 were treated with DMSO, 2 μM ascomycin (PP2B inhibitor), 20 nM calyculin A (PP1/PP2A inhibitor), or 100 nM okadaic acid (PP1/PP2A inhibitor) for 2 hr and immunoblotted as in (A). Graph shows pS-295 levels (divided by total PSD-95 level) (n = 3), normalized to untreated control. Statistical analysis was performed by one-way ANOVA, followed by the Dunnett's test. **$p < 0.01$, compared to DMSO control.

(E) In vitro phosphorylation of PSD-95 on ser-295 by recombinant JNK1. Purified hexahistidine-tagged fusion protein of PSD-95 (amino acids 41–355) was mixed with recombinant active JNK1 (see Experimental Procedures). After in vitro kinase reaction, protein samples were immunoblotted using pS-295 antibody, mouse PSD-95, and mouse JNK1 antibody, as indicated. Asterisk marks a mobility shift of His-tagged PSD-95 fusion protein after in vitro JNK1 kinase reaction.

(F) Phosphorylation of PSD-95 on ser-295 by JNK1 in COS-7 cells. Wild-type PSD-95 was transfected with vector control (pGW1-Myc) or JNK1. 30 hr later, transfected COS-7 cell lysates were immunoblotted with rabbit pS-295 antibody or rabbit pJNK antibody. After stripping, the blot was reprobed with mouse PSD-95 antibody or mouse myc antibody (9E10).

and 3B). Corroborating the biochemical result, TTX (2 μM, ~16 hr) robustly increased the brightness of dendritic pS-295 puncta; pS-295 immunostaining intensity per area of dendrite increased by >2-fold, compared to DMSO control (Figure 4B). Total PSD-95 staining intensity was also increased, but to a lesser degree (~40%). Since total level of PSD-95 in neuronal culture lysates was unchanged by western blotting during the same period of drug treatment (Figure 3A), the immunocytochemical result suggests a higher enrichment of PSD-95 at synapses associated with ser-295 phosphorylation. Conversely, bicuculline (25 μM, ~16 hr) strongly reduced pS-295 immunostaining intensity to ~25% of DMSO control, while total dendritic PSD-95 staining intensity fell to ~55% (Figure 4B). In addition to confirming the bidirectional regulation of phospho-ser-295 by activity, these immunocytochemical data

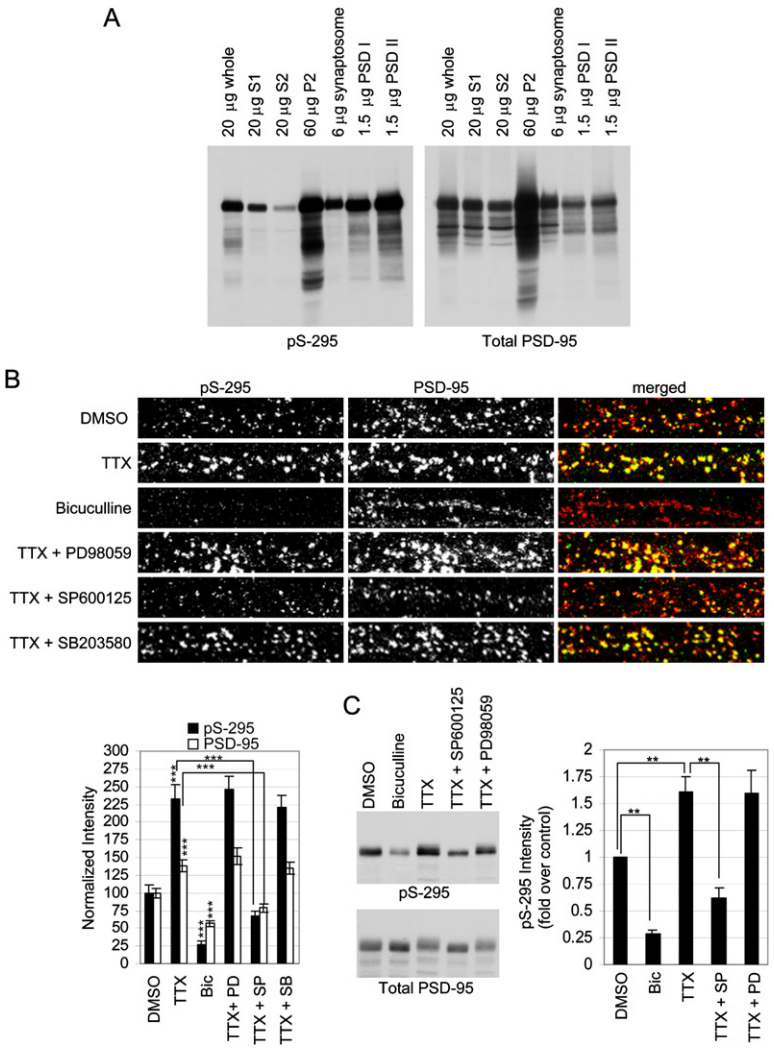


**Figure 4. PSD-95 Ser-295 Phosphorylation Is Bidirectionally Modulated by Neuronal Activity and Depends on JNK**

(A) Phospho-ser-295-PSD-95 is more enriched in postsynaptic density than total PSD-95. Subcellular and PSD fractions of rat forebrain were immunoblotted with pS-295 or PSD-95 antibody. Amount of protein loaded is indicated above each lane.

(B) Cultured hippocampal neurons (DIV24) were treated with either DMSO, 25 μM bicuculline, 2 μM TTX, 2 μM TTX plus PD98059 (25 μM), 2 μM TTX plus SP100126 (20 μM), or 2 μM TTX plus SB203580 (2.5 μM) for 16 hr before cold methanol fixation and double immunostaining with pS-295 (green) and PSD-95 (red) antibody. Individual channels are shown in grayscale. Quantified fluorescence intensity data are shown in the bar graph below. n = 20–25 microscope fields for each. ***$p < 0.001$, compared with DMSO control.

(C) Cultured hippocampal neurons (DIV24) were treated with either DMSO, 40 μM bicuculline, 2 μM TTX, 2 μM TTX plus PD98059 (25 μM), 2 μM TTX plus SP600125 (20 μM), or 2 μM TTX plus SB203580 (2.5 μM) for ~16 hr. Whole-cell lysates were immunoblotted with pS-295 or PSD-95 antibody. Bar graph shows pS-295 band intensity (divided by total PSD-95 in same lane) normalized to DMSO control (n = 4, **$p < 0.01$).

demonstrate that phospho-ser-295 levels correlate with the abundance of total PSD-95 in synapses. As a more subtle point, the larger amplitude fluctuation in pS-295 level versus total PSD-95 level implies that not all of synaptic PSD-95 is phosphorylated on ser-295 (i.e., nonphosphorylated PSD-95 is also present at synapses).

The TTX-induced increase of phospho-ser-295 and total PSD-95 immunostaining in dendrites was blocked by JNK inhibitor SP600125 (20 μM) but not by p38 inhibitor (SB203580, 2.5 μM) or ERK pathway inhibitor (PD98059, 25 μM) (Figure 4B). This result was backed up by immunoblot analysis, which showed that the TTX-induced increase of phospho-ser-295 PSD-95 is prevented by SP600125, but not by PD98059 (Figure 4C). Thus, JNK kinase activity is involved in regulation of ser-295 phosphorylation of endogenous PSD-95 at synapses.

## Knockdown of JNK1 Reduces Ser-295 Phosphorylation and Postsynaptic PSD-95 Levels

Which JNK isoform is important for ser-295 phosphorylation in neurons? JNK1 and JNK3 are the major isoforms of JNK in neurons (Brecht et al., 2005; Coffey et al., 2002). Transfection of a plasmid (JNK1-RNAi) that expresses a small hairpin RNA against JNK1 suppressed expression of endogenous JNK1, as measured by immunostaining with a JNK1 antibody (Figure 5A; arrows). JNK1 immunoreactivity in neurons was unaffected by JNK3-RNAi or the parent pSUPER vector (Figure 5A). In COS-7 cells, JNK1-RNAi reduced expression of cotransfected JNK1, but not JNK3 (Figure 5B). We tried to test the efficacy of JNK3-RNAi in neurons, but failed for technical reasons because two different JNK3 antibodies did not work in immunostaining of neurons. However, we were able to demonstrate the specific efficacy of JNK3-RNAi in COS-7 cells, where protein expression of rat JNK3 was inhibited by cotransfection of JNK3-RNAi but not JNK1-RNAi (Figure 5B).

We transfected JNK-RNAi constructs with β-gal marker into cultured hippocampal neurons at DIV14–15, and expressed for 3 days. Knockdown of endogenous JNK1 strongly reduced ser-295 phosphorylation of PSD-95 (to <20% of control), as assayed by pS-295 immunostaining intensity in transfected neurons (Figure 5C, quantified in

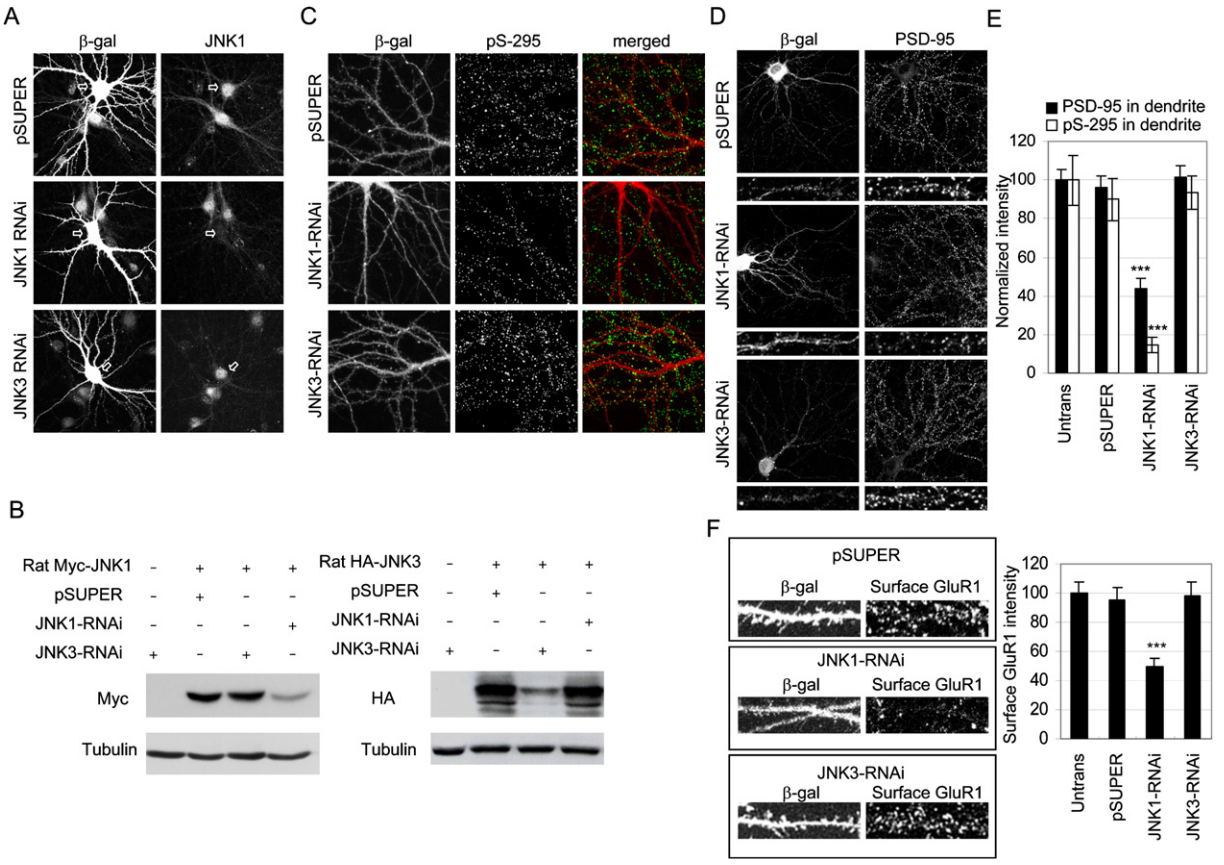


**Figure 5. RNAi Knockdown of Endogenous JNK1 Inhibits Ser-295 Phosphorylation and Reduces Synaptic PSD-95 Levels**

(A) Knockdown of endogenous JNK1 with JNK1-RNAi. Cultured hippocampal neurons at DIV14–15 were cotransfected with pSUPER, JNK1-RNAi, or JNK3-RNAi constructs plus β-gal marker (4:1 DNA ratio in favor of RNAi plasmid). Three days later, neurons were fixed and double stained with rabbit β-gal and mouse JNK1 antibody. Arrows point to soma of transfected neurons.

(B) Efficacy and specificity of JNK1 and JNK3-RNAi in COS-7 cells. COS-7 cells were cotransfected with indicated expression vectors, and immunoblotted 60 hr later for JNK1 (Myc), JNK3 (HA), and tubulin.

(C) Knockdown of endogenous JNK1 causes loss of phospho-ser-295 staining. Cultured hippocampal neurons at DIV14–15 were cotransfected with pSUPER, JNK1-RNAi, or JNK3-RNAi plus β-gal marker (4:1 ratio). Three days later, transfected neurons were double stained for β-gal (red) and phospho-ser-295 (green). Individual channels are shown in grayscale. N.B. In the JNKi-RNAi panel, pS-295 staining is mostly from untransfected dendrites crossing the field.

(D) Knockdown of endogenous JNK1 causes loss of postsynaptic PSD-95. Cultured hippocampal neurons at DIV14–15 were cotransfected with pSUPER, JNK1-RNAi, or JNK3-RNAi, plus β-gal. Three days later, transfected neurons were double labeled for β-gal and total PSD-95. Only single-channel images are shown.

(E) Quantitation of data from (C) and (D). Bar graph shows mean ± SEM of dendritic staining intensity of pS-295 and PSD-95, normalized to untransfected cells. n = 14–18 neurons for each. ***$p < 0.001$ compared with pSUPER or JNK3-RNAi.

(F) Knockdown of endogenous JNK1 causes loss of surface GluR1. Cultured hippocampal neurons at DIV14–15 were cotransfected with pSUPER, JNK1-RNAi, or JNK3-RNAi plus β-gal (4:1 ratio). Three days later, transfected neurons were double stained for β-gal and surface GluR1. Bar graph shows mean ± SEM of dendritic surface GluR1 intensity, normalized to untransfected cells. n = 15–20 neurons for each. ***$p < 0.001$ compared with pSUPER or JNK3-RNAi transfected neurons.

5E). Intensity of total dendritic PSD-95 staining was also significantly reduced, though to a lesser degree (~50%; Figures 5D and 5E). Neither total nor phospho-ser-295 PSD-95 was affected by control pSUPER or JNK3-RNAi transfection (Figures 5C–5E). These results suggest that JNK1, but probably not JNK3, is critically involved in phosphorylation of ser-295 of PSD-95 and in synaptic accumulation of PSD-95. In addition, surface GluR1 levels were reduced ~50% in neurons transfected with JNK1-RNAi but were unaffected by JNK3-RNAi or pSUPER alone (Figure 5F). An additional JNK1-RNAi construct (JNK1-RNAi #2) targeting a different sequence in JNK1 mRNA had similar effects on dendritic PSD-95 levels and surface GluR1 expression (data not shown).

## Knockdown of JNK1 Suppresses Basal Synaptic Transmission

We compared the effect of JNK1 RNAi and JNK3 RNAi on excitatory synaptic transmission in CA1 pyramidal neurons in hippocampal slice cultures (Figure S4). Knockdown of

JNK1 suppressed AMPA-EPSCs (0.44 ± 0.06-fold relative to untransfected). JNK1-RNAi also inhibited NMDA-EPSCs, though to a lesser extent (0.58 ± 0.07) (Figure S4A). JNK3-RNAi had no significant effect on AMPA- and NMDA-EPSCs (Figure S4B). These data are consistent with the idea that specifically JNK1 promotes the synaptic abundance of PSD-95 by phosphorylating ser-295. However, because RNAi knockdown of PSD-95 in cultured hippocampal slice reduces AMPA- but not NMDA-EPSCs (Elias et al., 2006; Nakagawa et al., 2004; Schluter et al., 2006), the inhibition of NMDA-EPSC by JNK1-RNAi is unlikely due to loss of PSD-95 alone. Thus, endogenous JNK1 activity is important for the maintenance of synaptic function, but perhaps involving substrates in addition to PSD-95.

### Rac1 Activity Promotes Ser-295 Phosphorylation

Small GTPases of the Rho family, particularly Rac1 and Cdc42, are important upstream regulators of JNK in various cell types (Hall, 2005; Weston and Davis, 2002). To determine whether a Rho family GTPase is involved in JNK-dependent phosphorylation of PSD-95 ser-295 in neurons, we expressed dominant-negative forms of Rac1 (Rac1-N17), Rac3 (Rac3-N17), Cdc42 (Cdc42-N17), RhoA (RhoA-N19), or RhoB (RhoB-N19) for 2 days (transfection at DIV15, fixation at DIV17). Among the constructs tested, only overexpression of Rac1-N17 reduced dendritic PSD-95 immunostaining (to ~40%; similar to RNAi of JNK1; Figure 6A). Rac1-N17 reduced dendritic pS-295 immunostaining by ~65%, whereas RhoA-N19 had no effect (Figure 6B). Surprisingly, Rac3-N17, which is 92% identical to Rac1, had little effect on dendritic PSD-95 levels (Figure 6A). These data demonstrate that PSD-95 phosphorylation on ser-295 depends on Rac1, consistent with a Rac1-JNK1 signaling pathway leading to ser-295 phosphorylation.

A recently developed inhibitor of Rac1 (NSC23766) is selective for Rac1 over Cdc42 and RhoA (Gao et al., 2004). Cultured hippocampal neurons at DIV25 were treated with bicuculline (25 μM), TTX (2 μM), or TTX (2 μM) plus Rac1-inhibitor (NSC23766, 100 μM) for ~16 hr and immunoblotted for phospho-ser-295-PSD-95 and phospho-JNK (Figure 6C). The TTX-induced increase of ser-295 phosphorylation was blocked by NSC23766 Rac1-inhibitor, without any concomitant effect on total PSD-95 levels (Figure 6C), showing that Rac1 activity is important for regulated ser-295 phosphorylation in neurons. However, these results do not prove that TTX increases ser-295 phosphorylation via stimulation of Rac1. Chronic treatment (~16 hr) with TTX or bicuculline had no detectable effect on total JNK activation levels, as judged by phospho-JNK immunoblotting (Figure 6C). NSC23766 (100 μM) alone for 16 hr reduced phospho-ser-295 PSD-95 levels and phospho-JNK levels by ~50% (Figure S5), suggesting that Rac1 is a major activator of JNK in neurons.

Finally, we turned to RNAi knockdown of endogenous Rac1 in cultured hippocampal neurons. When cotransfected in COS-7 cells, the Rac1-RNAi construct reduced Rac1 protein expression, but had no effect on the highly homologous Rac3 protein (Figure 6D) or RhoA (data not shown). Consistent with dominant-negative Rac1-N17 and pharmacological Rac1-inhibitor results, RNAi knockdown of endogenous Rac1 caused loss of dendritic PSD-95 staining, whereas control pSUPER or RhoA-RNAi transfection had no effect (Figure 6E). Knockdown of Rac1 also strongly reduced phospho-ser-295 staining in cultured neurons (Figure S6). Together, these data indicate that Rac1 is an important regulator of JNK in neurons and required for ser-295 phosphorylation and synaptic accumulation of PSD-95. The data are consistent with a Rac1-JNK1 signaling pathway that controls ser-295 phosphorylation and hence PSD-95 content at postsynaptic sites. However, it is also possible that the loss of dendritic PSD-95 with dominant-negative Rac1-N17 is secondary to disturbance of synapse growth or maintenance, because Rac1 is also known to promote spine morphogenesis via regulation of the actin cytoskeleton (Nakayama et al., 2000; Tashiro et al., 2000). In our mature dissociated culture preparation, the expression of dominant-negative Rac1 (Rac1-N17) or Rac1-RNAi construct for 3 days led to a small reduction in density of dendritic protrusions and thinner longer spines (Figure S7).

### Bidirectional Regulation of Ser-295 Phosphorylation in Chemical LTD and Chemical LTP

Synaptic excitation induced by bicuculline reduces ser-295 phosphorylation on a time scale of minutes (Figure 3C). Which glutamate receptor might mediate suppression of ser-295 phosphorylation? In cultured hippocampal neurons, the NMDA receptor blocker DL-APV (100 μM; 45 min) significantly increased phospho-ser-295-PSD-95 levels (Figure S8). The AMPA receptor antagonist NBQX (10 μM; 45 min) had no significant effect (Figure S8). We conclude that NMDA receptor activation plays a dominant role in suppressing ser-295 phosphorylation.

Bath application of NMDA for short time periods is widely used to induce "chemical LTD" in cultured neurons and brain slices (Lee et al., 1998). NMDA treatment (75 μM) of cultured hippocampal neurons caused a profound fall in phospho-ser-295-PSD-95 levels within 5 min (Figure 7A). Thus, acute stimulation of NMDA receptors can rapidly dephosphorylate PSD-95 on ser-295. We measured Rac1 activity (by GST-PAK1-PBD [p21-binding domain] pulldown assay) and PP1/PP2A activity (see Experimental Procedures) in cultured neurons stimulated with NMDA. We focused on PP1/PP2A activity because these phosphatases seem to regulate basal phosphorylation on ser-295 (see Figure 3D). GTP-Rac1 levels did not change significantly after NMDA stimulation (5–10 min) or APV treatment (Figure 7B). Phospho-JNK levels also were unaffected by short-term NMDA treatment (data not shown). PP1/PP2A phosphatase activity, however, increased significantly following the same NMDA stimulation

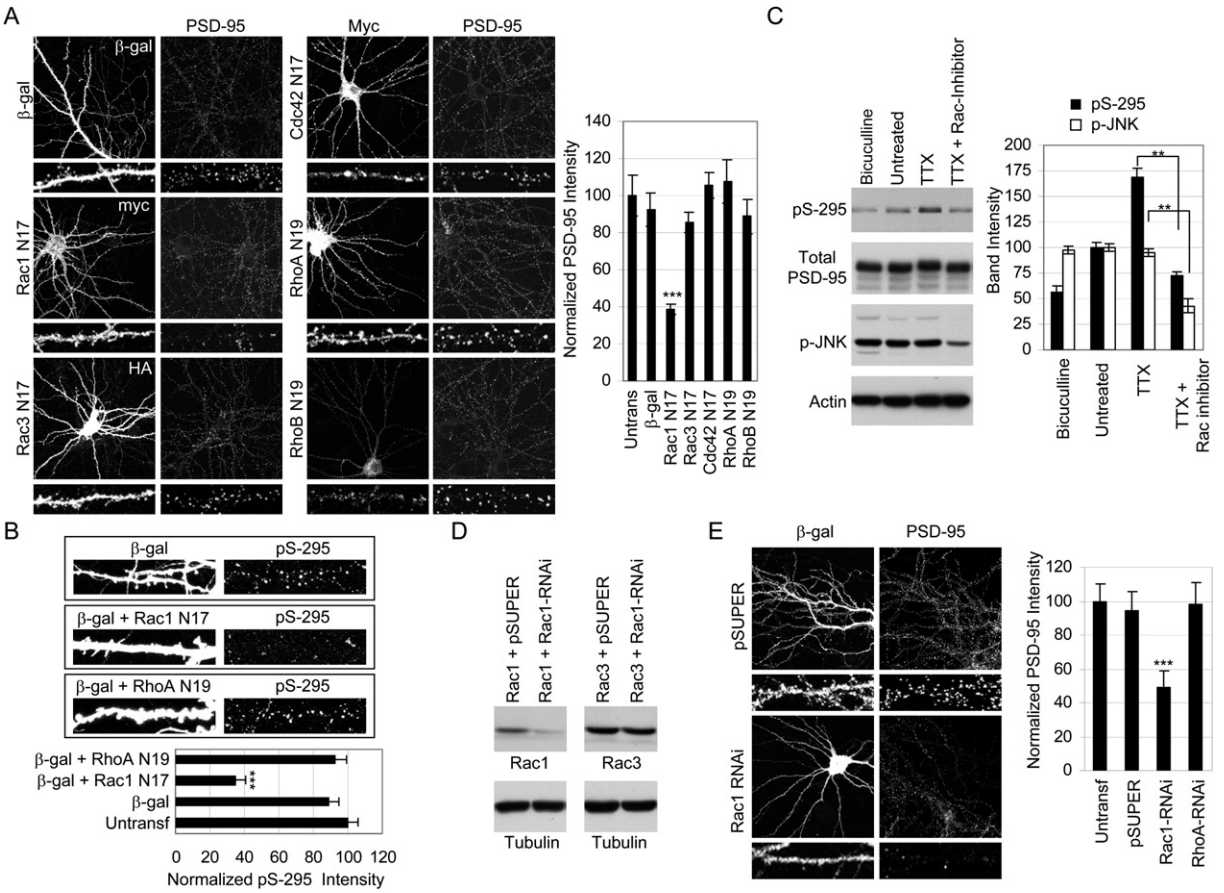


**Figure 6. Inhibition of Rac1 Reduces Ser-295 Phosphorylation and Synaptic PSD-95 Levels**

(A) Effects of dominant-negative Rho family GTPases on dendritic PSD-95. Neurons were transfected at DIV15 with dominant-negative constructs of specific Rho GTPases or β-gal, as indicated, and stained 2 days later for PSD-95. Bar graph shows mean ± SEM of dendritic PSD-95 staining intensity, normalized to untransfected cells. n = 15–18 neurons for each. ***$p < 0.001$, compared with untransfected neurons or β-gal-transfected neurons.

(B) Expression of Rac1-N17 causes loss of phospho-ser-295 staining. Cultured hippocampal neurons at DIV15 were cotransfected with β-gal, β-gal plus Rac1-N17, or β-gal marker plus RhoA-N19 (1:4 ratio). Two days later, transfected neurons were double stained for β-gal and phospho-ser-295. Graph shows show mean ± SEM of dendritic pS-295 staining intensity, normalized to untransfected cells. n = 20 neurons for each. ***$p < 0.001$, compared with untransfected neurons or neurons transfected with β-gal or βgal plus RhoA-N19.

(C) Effect of Rac1-inhibitor (NSC23766) on ser-295 phosphorylation and phospho-JNK levels. Cultured hippocampal neurons at DIV25 were untreated or treated with bicuculline (25 μM), TTX (2 μM), or TTX plus Rac-inhibitor (NSC23766, 100 μM, Calbiochem) for ~16 hr. Cell lysates were immunoblotted with pS-295, PSD-95, or phospho-JNK antibody. Bar graph shows mean ± SEM of band intensities, normalized to untreated. n = 4. **$p < 0.01$.

(D) Specificity and efficacy of Rac1-RNAi in COS-7 cells. COS-7 cells were transfected with expression vectors for myc-Rac1 or myc-Rac3, plus pSUPER vector or Rac1-RNAi constructs, as indicated, and immunoblotted 60 hr later for myc and tubulin.

(E) Knockdown of endogenous Rac1 causes depletion of synaptic PSD-95. Cultured hippocampal neurons at DIV15–16 were cotransfected with pSUPER, Rac1-RNAi, or RhoA-RNAi construct, plus β-gal marker (4:1 ratio). Three days later, transfected neurons were double stained for β-gal and PSD-95. Bar graph shows mean ± SEM of dendritic PSD-95 intensity, normalized to untransfected. n = 28 neurons for each. ***$p < 0.001$.

(Figure 7C), suggesting that increased PP1/PP2A activity may be responsible for NMDA-induced dephosphorylation of ser-295.

We then investigated whether PSD-95 ser-295 phosphorylation is affected in a "chemical LTP" protocol (cultured hippocampal neurons treated with forskolin/rolipram /0 Mg2+ [see Experimental Procedures]), which is known to increase synaptic strength and drive AMPA receptors to the surface (Oh et al., 2006; Otmakhov et al., 2004). In contrast to the rapid dephosphorylation induced by NMDA treatment (chemical LTD), ser-295 phosphorylation was increased by the chemical LTP protocol, occurring over ~25–50 min (Figure 7D, 7E2, compare with 7A). The time course of PSD-95 ser-295 phosphorylation was somewhat delayed compared to the time course of GluR1 ser-845 phosphorylation and activation of ERK1/2 (phospho-ERK), which were also induced following chemical LTP (Figures 7D, 7E1, and 7E3). The chemical LTP protocol raised phospho-JNK (Figures 7D and 7E4) and GTP-Rac1 levels in the cultured neurons (Figure 7F),

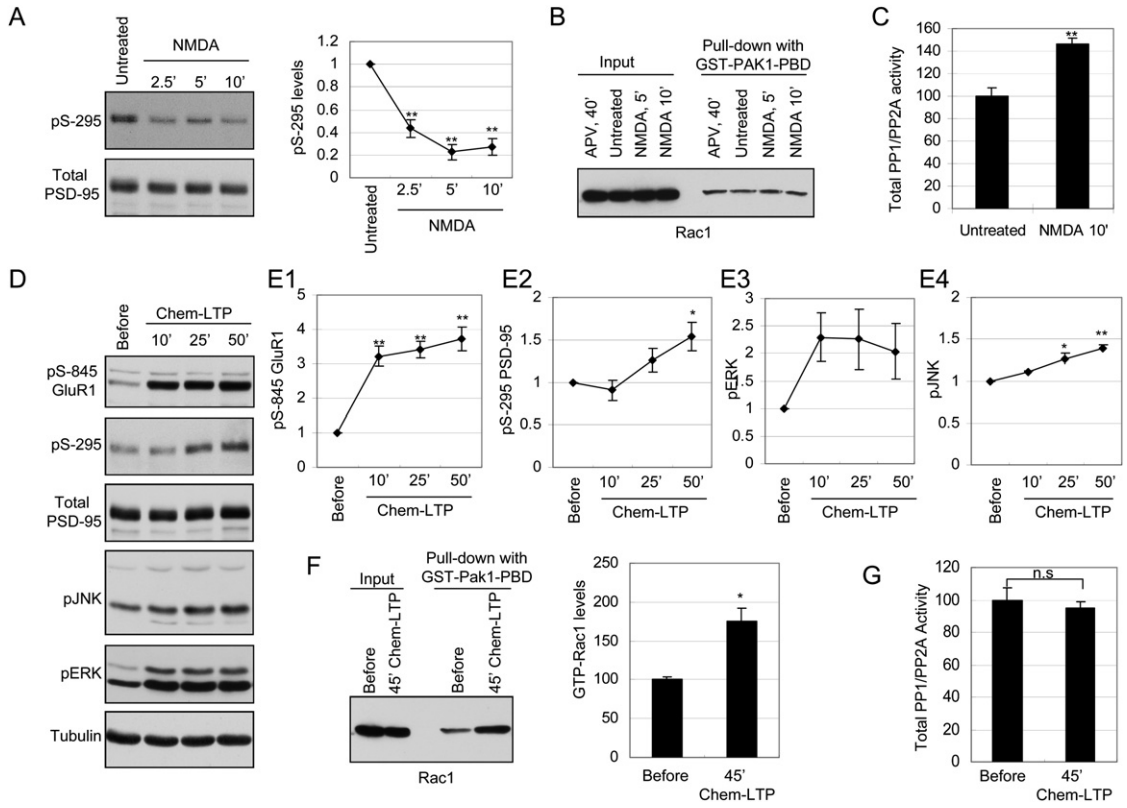


**Figure 7. Bidirectional Regulation of Phospho-Ser-295 Levels by NMDA Treatment and Chemical LTP Induction**

(A) NMDA treatment induces rapid dephosphorylation of ser-295. Cultured hippocampal neurons at DIV 24–27 were stimulated with NMDA (75 μM) for indicated times. Levels of phospho-ser-295 of PSD-95 were analyzed by immunoblotting with pS-295 antibody. After stripping, the blot was reprobed with mouse PSD-95 antibody. Graphs show time course of pS-295 band intensity (divided by total PSD-95) after NMDA stimulation (n = 4; normalized to untreated control). **p < 0.01, compared to untreated control; one-way ANOVA, followed by the Dunnett's test.

(B) Lack of effect of APV and NMDA treatment on Rac1-GTP levels. Cultured hippocampal neurons at DIV24–27 were untreated or treated with APV (100 μM, 40 min) or NMDA (75 μM for indicated times). Levels of GTP-Rac1 were analyzed by GST-PAK1-PBD pulldown assay. A representative immunoblot from three independent experiments is shown.

(C) NMDA treatment increases PP1/PP2A phosphatase activity. Cultured hippocampal neurons at DIV 27 were untreated or stimulated with NMDA (75 μM) for 10 min, and equal amounts of cell lysate protein were analyzed by the Malachite Green PP1/PP2A phosphatase assay (see Experimental Procedures). PP1/PP2A phosphatase activity was normalized to untreated control. Bar graph shows mean ± SEM of four sets of experiments. **p < 0.01.

(D) Representative immunoblots showing effects of chemical LTP induction on PSD-95 ser-295 phosphorylation, GluR1 ser-845 phosphorylation, phospho-ERK, and phospho-JNK. Cultured hippocampal neurons at DIV24–28 were treated with 50 μM forskolin and 0.1 μM rolipram in ACSF lacking $MgCl_2$ (see Experimental Procedures). After 10 min, neurons were replaced in regular ACSF and then immunoblotted at indicated time points, using indicated antibodies.

(E1–E4) Time course of (E1) GluR1 pS-845 levels (divided by tubulin level; n = 6), (E2) pS-295 levels (divided by total PSD-95 level; n = 6), (E3) pERK (divided by tubulin; n = 3), and (E4) pJNK (divided by tubulin; n = 4) after chemical LTP induction. Statistical analysis was performed by one-way ANOVA, followed by the Dunnett's test. **p < 0.01; *p < 0.05, compared to samples before treatment with 50 μM forskolin/0.1 μM rolipram/0 $MgCl_2$.

(F) Effect of chemical LTP induction on Rac1-GTP levels. 45 min after chemical LTP induction as above, GTP-Rac1 was measured by GST-PAK1-PBD pulldown assay. Graph shows mean ± SEM of Rac1-GTP levels, *p < 0.05, t test; n = 3.

(G) Effect of chemical LTP induction on PP1/PP2A phosphatase activity. Graph shows mean ± SEM of PP1/PP2A phosphatase activity, normalized to sample before treatment with 50 μM forskolin/0.1 μM rolipram/0 $MgCl_2$. n = 3, p > 0.05, t test.

consistent with the idea that ser-295 phosphorylation is upregulated by the Rac1-JNK pathway. In contrast to chemical LTD (Figure 7C), total PP1/PP2A phosphatase activity was unaffected by the chemical LTP protocol (Figure 7G). In short, phosphorylation of PSD-95 ser-295 is rapidly and bidirectionally regulated in neurons: it is induced by chemical LTP, associated with enhanced Rac1 and JNK activity, and inhibited by chemical LTD, associated with elevated PP1/PP2A phosphatase activity.

Chronic treatment with bicuculline (25 μM, ~16 hr) led to a significant reduction of GTP-Rac1 (Figure S9), suggesting that bicuculline reduces phospho-ser-295 PSD-95 levels by inhibiting the Rac1-JNK pathway (see Figure 3). TTX treatment (2 μM, 16 hr) showed a trend toward increased Rac1-GTP levels, but this did not reach statistical significance. No change in total PP1/PP2A activity was observed after ~16 hr treatment with TTX or bicuculline (Figure S9).

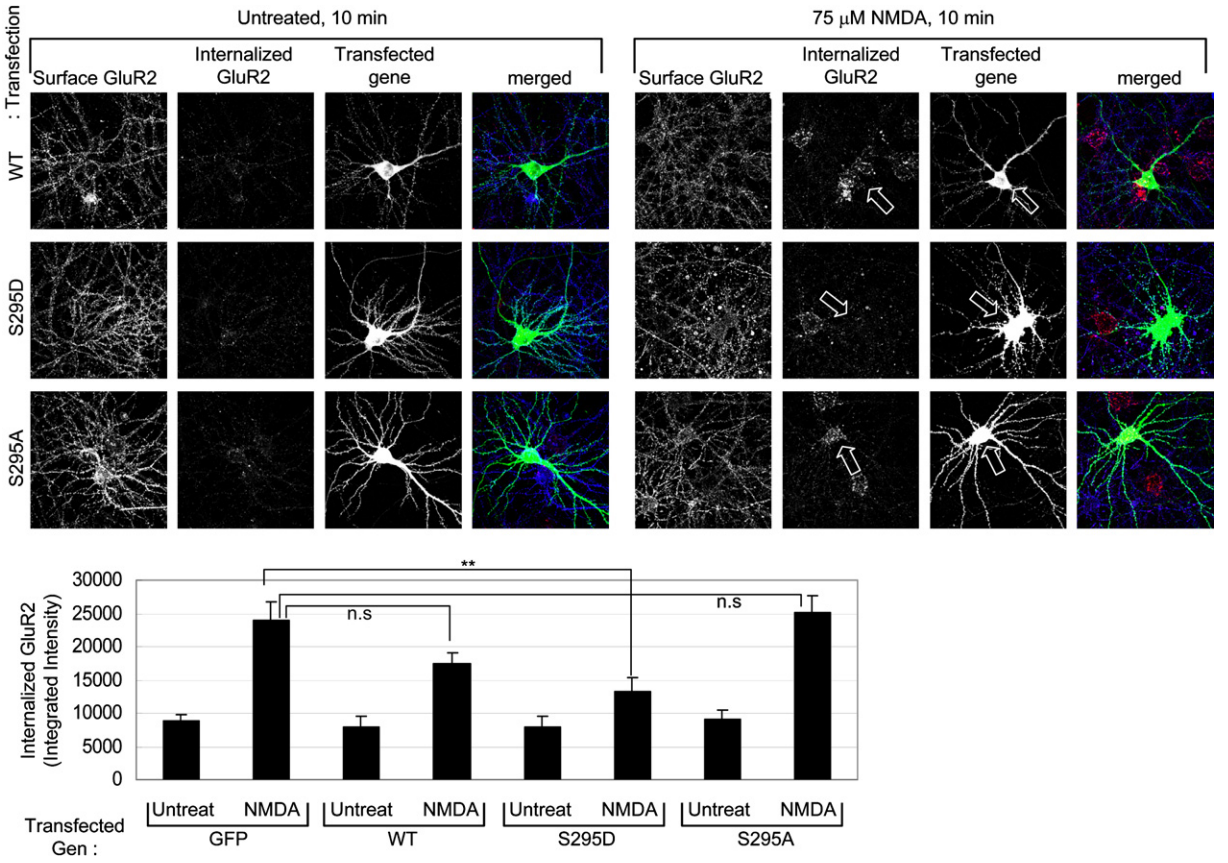


**Figure 8. Overexpression of S295D PSD-95 Inhibits NMDA-Induced GluR2 Internalization**

Cultured hippocampal neurons were transfected with GFP, WT-PSD-95-GFP, S295D-PSD-95-GFP, or S295A-PSD-95-GFP at DIV16. Three days later (DIV19), surface GluR2 was live-labeled with GluR2-N Ab, washed, and then were left untreated or treated with 75 μM NMDA for 10 min at 37°C. Internalized GluR2 receptors and remaining surface GluR2 receptors were visualized with Alexa-568 (red) and Alexa-647 (blue) secondary antibody, respectively (see Experimental Procedures). Transfected neurons were identified with GFP-channel (green). Bar graph shows mean ± SEM of integrated intensity of internalized GluR2 receptor. n = 11, 10, 9, 15, 13, 18, 9, and 17 from left to right. **$p < 0.01$, compared with neurons transfected with GFP. There was no difference in the GluR2 internalization between S295A-PSD-95 and GFP-transfected neurons ($p > 0.05$).

### Overexpression of S295D-PSD-95 Mutant Blocks AMPA Receptor Internalization and LTD

NMDA bath application is well known to stimulate AMPA receptor internalization. We found that overexpression of the phosphomimicking S295D-PSD-95 mutant in cultured hippocampal neurons inhibited GluR2 internalization induced by NMDA, whereas S295A-PSD-95 mutant had no effect (Figure 8). Wild-type PSD-95 overexpression showed a trend toward inhibiting NMDA-induced GluR2 internalization, but this did not reach statistical significance. These results suggest that ser-295 dephosphorylation of PSD-95 plays a functional role in inducible AMPA receptor internalization.

The inhibition of NMDA-induced AMPA receptor internalization by S295D-PSD-95 raised the question of whether this phosphomimicking mutant would inhibit LTD. To address this issue, we overexpressed the PSD-95 mutant constructs with GFP marker in CA1 neurons of cultured hippocampal slices (as in Figure 2), and investigated LTD of Schaffer collateral-CA1 synapses in whole-cell recording mode (Figure 9). Overexpression of S295D-PSD-95 blocked induction of LTD (96% ± 7% of baseline, n = 8), whereas overexpression of S295A-PSD-95 had no effect (63% ± 5% of baseline, n = 8). There was no difference in the magnitude of LTD between control untransfected cells and cells transfected with S295A-PSD-95. It should be noted that the loss of LTD in S295D-expressing neurons occurred despite an elevated basal synaptic transmission (see Figure 2); therefore, it cannot be attributed to "occlusion" of LTD. These results suggest that dephosphorylation of ser-295 of PSD-95 is critical for LTD induction.

## DISCUSSION

### Regulation of PSD-95 by Ser-295 Phosphorylation

Altering the abundance of the PSD-95 scaffold at synapses is a primary means to control PSD-95 function and

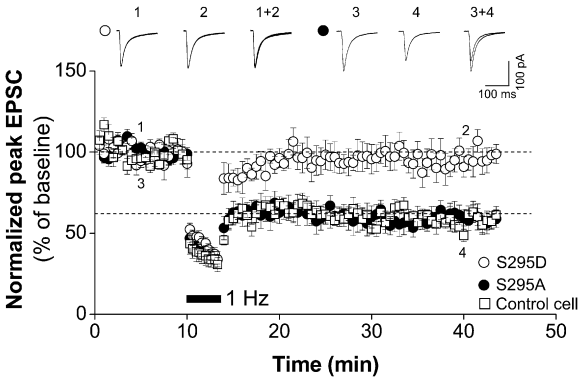


**Figure 9. Overexpression of S295D-PSD-95 Blocks LTD in CA1 Neurons of Organotypic Hippocampal Slice Cultures**

CA1 neurons were biolistically transfected with S295D-PSD-95 or S295A-PSD-95 (cotransfected with GFP) and recorded in whole-cell patch-clamp mode. Induction of LTD was blocked in cells overexpressing S295D-PSD-95 ($p > 0.05$, comparison between 5 min and 40 min, n = 8). LTD was intact in S295A-PSD-95-transfected CA1 neurons from organotypic hippocampal culture ($p < 0.01$, comparison between 5 min and 40 min, n = 8). There was no difference in the magnitude of LTD between S295A-PSD-95-transfected and nontransfected control neurons ($p > 0.05$).

synaptic strength. Consistent with this idea, synaptic activity leads to depalmitoylation of PSD-95, which is correlated with depletion of synaptic PSD-95 clusters, loss of AMPA receptors, and weakening of synapses (El-Husseini et al., 2002). Activity-induced ubiquitination of PSD-95 and subsequent loss of PSD-95 from synapses by proteasomal degradation is also implicated in synaptic depression (Colledge et al., 2003). Our study reveals a mechanism for controlling synaptic abundance of PSD-95 based on phosphorylation and dephosphorylation of a specific residue of PSD-95. Phosphorylation of ser-295 occurs in vivo, and it enhances the ability of PSD-95 to accumulate in the PSD, to recruit surface AMPA receptors, and to strengthen synaptic transmission.

Phosphorylation of ser-295 of PSD-95 is bidirectionally regulated—it is inhibited by bicuculline and chemical LTD but enhanced by TTX and chemical LTP. Ser-295 phosphorylation correlates with increased accumulation of phosphorylated and total PSD-95 at synapses, which would be expected to promote synaptic strength. The relative importance of ser-295 phosphorylation versus N-terminal palmitoylation is unknown with respect to synaptic localization of PSD-95. It is possible that ser-295 phosphorylation influences palmitoylation or vice versa, but this is somewhat difficult to envisage since the N-terminal cysteines and ser-295 are widely separated, at least in primary structure.

Previous reports indicated that the effect of PSD-95 overexpression on synaptic function is not activity dependent (i.e., occurs in the presence of high $Mg^{2+}$) (Ehrlich and Malinow, 2004), which seems to be in superficial conflict with our findings. However, ser-295 phosphorylation is not absolutely required for synaptic potentiation, as indicated by the 3-fold enhancement of AMPA-EPSCs by S295A-PSD-95 overexpression. Ser-295 phosphorylation also seems not absolutely necessary for PSD-95 to reach the synapse, since (1) S295A-PSD-95 is present in spines (albeit less concentrated than wild-type or S295D mutant); (2) total PSD-95 levels at synapses fluctuate with activity at a smaller amplitude than phospho-ser-295-PSD-95, implying that ser-295-phosphorylated PSD-95 is only a subset of synaptic PSD-95; (3) S295A-PSD-95 does not act as a dominant-negative mutant in AMPA-EPSC potentiation. The simplest explanation is that phosphorylation of PSD-95 at ser-295 enhances PSD-95 stability, and hence accumulation, at synapses, but phosphorylation itself is not essential for targeting to synapses. Especially upon overexpression (when it is unlikely to be stoichiometrically regulated by activity-dependent phosphorylation), PSD-95 would be expected to potentiate synaptic transmission whether or not activity is inhibited.

Ser-295-phosphorylated PSD-95 is more enriched in PSD fractions than total PSD-95, and S295D-PSD-95 had a more potent effect on surface GluR1 levels and AMPA EPSCs. These data argue that S295D-PSD-95 is more synaptically enriched. An unanswered question is: how does phosphorylation of ser-295 promote synaptic accumulation of PSD-95? We do not believe that ser-295 regulates degradation of PSD-95, because the degree of ser-295 phosphorylation can change drastically with little effect on total PSD-95 protein levels. Broadly speaking, ser-295 phosphorylation could either facilitate the delivery of PSD-95 to the synapse (e.g., by being engaged in motor trafficking), or it could increase the stability of PSD-95 at the synapse (for instance, by strengthening PSD-95 interactions with other PSD proteins).

Ser-295 resides in a "linker" of 67 amino acids between PDZ domains 2 and 3, where it seems unlikely to influence the binding interactions mediated by the PDZ or other well-characterized domains of PSD-95. It is possible that phosphorylation of ser-295 alters local protein conformation such that a yet-to-be identified protein-protein interaction is enhanced, thereby stabilizing PSD-95 in the PSD. Whatever the underlying molecular mechanism, it is interesting that PSD-93, a close relative of PSD-95, also possesses a similar phosphorylation motif in the PDZ2-PDZ3 linker region (Jaffe et al., 2004; Trinidad et al., 2006). Other phosphorylation sites have been identified in PSD-95 that are phosphorylated by CDK5 and CaMKII (Gardoni et al., 2006; Morabito et al., 2004), but their significance is not clear.

## Signal Transduction Pathway Underlying Regulated PSD-95 Ser-295 Phosphorylation

Our data point to the Rac1-JNK1 pathway as being the main mediator of ser-295 phosphorylation. The dephosphorylation of PSD-95 ser-295 seems to involve the phosphatases PP1 and/or PP2A. Our findings indicate that different stimuli utilize different signaling mechanisms to regulate phospho-ser-295 PSD-95 levels in neurons.

NMDA stimulation (chemical LTD) induced dephosphorylation of PSD-95 ser-295 within minutes, correlated with elevated PP1/PP2A phosphatase activity but unaltered Rac1 or total JNK activity. We note that PP1 activation and recruitment to stimulated synapses is required for LTD (Morishita et al., 2001; Mulkey et al., 1994), raising the question of whether PSD-95 is a critical substrate of PP1 in synaptic depression. In contrast, chemical LTP stimulated phosphorylation on ser-295, associated with elevated Rac1/JNK activity but no change in PP1/PP2A. These results underscore the bidirectional regulation of phospho-ser-295-PSD-95 levels in neurons, and the different ways it can be achieved via controlling the balance of activities of the Rac1-JNK kinase pathway and PP1/PP2A phosphatases.

## Physiological Role of Ser-295 Phosphorylation

Ser-295 phosphorylation of PSD-95 is regulated acutely, i.e., within 5 min of chemical LTD and within 50 min of chemical LTP stimulation, as well as chronically, i.e., in response to prolonged alterations in activity levels (16 hr TTX or bicuculline). Since ser-295 phosphorylation promotes PSD-95 localization in synapses, the rapid dephosphorylation of this site would favor the loss of PSD-95 from synapses following LTD-inducing stimuli, which has been observed previously (Colledge et al., 2003). We found that overexpression of the S295D-PSD-95 mutant, which mimics phosphorylation and cannot be "dephosphorylated," blocks induction of LTD. The simplest interpretation of these data is that dephosphorylation of PSD-95 ser-295 is critical for LTD, presumably because this dephosphorylation is required for dispersal of PSD-95 from synaptic sites and subsequent mobilization and internalization of AMPA receptors. In support of this hypothesis, overexpression of S295D-PSD-95, but not wild-type or S295A mutant, inhibits NMDA-induced AMPA receptor internalization. A caveat of these experiments is that the PSD-95 mutants are overexpressed, so this interpretation should be further tested by a knockin of the ser-295 mutation in the genome. In addition, because the S295D mutant accumulates more in the synapse, we cannot exclude the possibility that LTD is blocked simply by a higher postsynaptic content of PSD-95, rather than by specific inability of S295D-PSD-95 to undergo dephosphorylation.

Chronic changes in the abundance of postsynaptic PSD-95 regulated by ser-295 phosphorylation could contribute to homeostatic plasticity (synaptic scaling) (Turrigiano and Nelson, 2004). Like synaptic scaling, total PSD-95 content of synapses is regulated by activity over a time course of many hours, correlating with phospho-ser-295 levels. Homeostatic synaptic scaling is at least partly mediated by postsynaptic changes in glutamate receptor content (Turrigiano and Nelson, 2004). Accumulation of PSD-95 through increased ser-295 phosphorylation could contribute to increased postsynaptic AMPA receptors during chronic inactivity (TTX) conditions.

## EXPERIMENTAL PROCEDURES

### pS-295 PSD-95 Phosphoantibody

Phosphopeptide (incorporating a cysteine residue at the N terminus) of sequence CSPRRY(pS)PVAKD conjugated to hemocyanin was used to immunize New Zealand White rabbits (Covance). For affinity purification of the pS-295 PSD-95 antibody, antiserum was passed through a SulfoLink column (Pierce) coupled with the nonphosphorylated peptide (CSPRRYSPVAKD). Pass-through fractions were subsequently purified on a SulfoLink column coupled with the phosphorylated peptide. After washing with Tris-buffered saline, bound antibody was eluted with 0.1 M glycine (pH 2.7).

### Chemical LTP Induction

Cultured hippocampal neurons were incubated for 20 min at room temperature in ACSF (in mM): 125 NaCl, 2.5 KCl, 1 $MgCl_2$, 2 $CaCl_2$, 33 D-glucose, and 25 HEPES (pH 7.3), then treated with 50 μM forskolin and 0.1 μM rolipram in ACSF lacking $MgCl_2$. After 10 min of stimulation, neurons were replaced in ACSF containing 1 mM $MgCl_2$ and lysed with 2× SDS sample buffer at indicated time points.

### In Vitro Kinase Assay

$His_6$-tagged fusion protein of PSD-95 (aa 41–355 of rat PSD-95) was expressed in *E. coli* BL21(DE3) and purified with $Ni^{2+}$-NTA-Agarose (QIAGEN). Purified protein (50 ng in 25 μl of reaction volume) was incubated at 30°C for 20 min in kinase buffer containing 50 mM Tris-HCl, pH 7.5, 0.1 mM EGTA, 0.1% 2-mecaptoethanol, 5 mM HEPES, pH 7.4, 10 mM magnesium acetate, 2 mM $CaCl_2$, and 0.1 mM ATP, with constitutive active recombinant JNK1 (100 ng; Upstate Biotechnology). Phosphorylation at serine-295 of PSD-95 was detected by immunoblotting with pS-295 antibody.

### Total PP1/PP2A Phosphatase Activity Assay

Total PP1/PP2A activity was measured using a Malachite Green PP1/PP2A Phosphatase Assay kit (Upstate Biotechnology), which is optimized for PP1 and PP2A, but cannot distinguish between these two enzymes. The assay is based on dephosphorylation of a phosphopeptide substrate (K-R-pT-I-R-R); the released phosphate binds to malachite green, leading to increased absorbance at 650 nm. Cultured hippocampal neurons were washed with ice-cold Tris-buffered saline, scraped into phosphatase extraction buffer (20 mM imidazol-HCl, 2 mM EDTA, pH 7.0, with 10 μg/ml of aprotinin, leupeptin, 1 mM benzamidine, and 1 mM PMSF) and then sonicated twice for 10 s. Resulting cell lysates (equal amounts of protein) were used for phosphatase activity assay. Absorbance values at 650 nm were subtracted by that of negative control (no cell lysate added).

### Rac1 Activation Assay

The active (GTP-bound) form of Rac1 was detected using EZ-Detect Rac1 Activation kit (Pierce, Rockford, IL), which is based on specific pulldown of Rac1-GTP by GST-PAK1-PBD (p21-binding domain), which contains the Rac1-GTP binding domain of Rac1 effector PAK1. Hippocampal neurons were lysed with cold MLB (25 mM Tris-HCl, pH 7.5, 150 mM NaCl, 5 mM $MgCl_2$, 1% NP-40, 1 mM DTT, and 5% glycerol). Equal amounts of protein from cleared cell lysates were incubated with beads charged with GST-PAK1-PBD for 1 hr at 4°C. Beads were washed with cold MLB three times. Bound proteins were eluted by 2× SDS sample buffer, and immunoblotted for Rac1 using monoclonal antibody included in the assay kit (Pierce).

### Image Acquisition and Quantification

Confocal images of neurons were obtained using a Zeiss 63× (NA 1.4) objective with sequential acquisition settings at the maximal resolution of the confocal (1024 × 1024 pixels). The confocal microscope settings were kept the same for all scans when fluorescence intensity was compared. All measurements were performed using ImageJ (NIH) software. For the surface AMPA receptor and bassoon quantification,

outlines of dendrites from transfected and untransfected cells were carefully traced. Fluorescence intensity was then determined for the traced areas. Staining intensity measurements are expressed in arbitrary units of fluorescence per square area. All values in figures and text refer to mean ± SEM unless otherwise stated. N refers to number of cells unless otherwise indicated. Statistical analysis of nonelectrophysiological data was performed with Student's t test.

### Electrophysiology

Electrophysiological recordings were carried out in organotypic slice cultures of rat hippocampus as described (Nakagawa et al., 2004). Neurons were transfected using biolistic gene gun (BioRad) at DIV4–6 {total 100 μg DNA; at a ratio of 9:1 (construct to test/marker pEGFP-C1 [Clontech]) for the overexpression of PSD-95 and its variants, and at a ratio of 9:1 (RNAi construct to test/marker pEGFP-C1) for the RNAi experiments}. Electrophysiological recordings were performed 3 days (overexpression experiment) or 5 days (RNAi experiment) after transfection. Recordings were carried out in solution containing (mM): NaCl 119, KCl 2.5, $CaCl_2$ 4, $MgCl_2$ 4, $NaHCO_3$ 26, $NaH_2PO_4$ 1, glucose 11, picrotoxin 0.15, and 2-chloroadenosine 0.01, gassed with 5% $CO_2$/95% $O_2$, at pH 7.4. Patch recording pipettes (2–4 M ohms) were filled with internal solutions containing (in mM): 115 cesium methanesulfonate, 20 CsCl, 10 HEPES, 2. 5 $MgCl_2$, 4 ATP disodium salt, 0.4 GTP trisodium salt, 10 sodium phosphocreatine, and 0.6 EGTA, at pH 7.25. For basal synaptic transmission, whole-cell recordings were made simultaneously from a pair of neighboring CA1 pyramidal neurons, one transfected and the other untransfected, while stimulating presynaptic fibers at 0.2 Hz. Synaptic AMPA receptor responses were recorded at –60 mV and NMDA receptor responses at +40 mV in the presence of NBQX (0.01 mM). Experiments were done blind to the DNA constructs used. Results are reported as mean ± SEM. Statistical significance was evaluated by Mann-Whitney test for EPSC amplitude, Kruskal-Wallis ANOVA for Figure 2D.

For LTD experiments, hippocampal slice cultures were prepared from 7-day-old rats and cultured for 6–8 days in vitro. Neurons were transfected at DIV3 (100 μg DNA; 90% of the construct to test; 10% pEGFP-C1) and recorded 3–5 days after transfection. Stimulation was delivered to Schaffer collateral-CA1 input every 15 s (0.033 Hz each input). EPSC amplitude, series resistance, and input resistance were monitored and analyzed on-line and off-line using the LTP program (Anderson and Collingridge, 2001). Only cells with series resistance <25 MΩ with a change in series resistance <10% from the start were included in this study. Synaptic AMPA receptor responses were recorded at −70 mV. Stimulation intensity was set between 5–15 V to produce 50%–70% of maximal response. A stable baseline recording for 10 min was required prior to any experimental manipulation. To induce LTD, 1 Hz stimulation (200 stimuli) at −40 mV was delivered. During 1 Hz stimulation, averages were made of 20 consecutive sweeps, and the other input was not stimulated. Data pooled across experiments are expressed as the mean ± SEM, and effects of conditioning stimulation were measured between 20–25 min after induction of LTD. Significance was tested using the Student's two-tailed t test.

Additional experimental procedures are described in Supplemental Data.

### Supplemental Data

The Supplemental Data for this article can be found online at http://www.neuron.org/cgi/content/full/56/3/488/DC1/.

## ACKNOWLEDGMENTS

We thank Potus Aspenstrom for Rac1-N17, Rac3-N17, Cdc42-N17, RhoA-N19, and RhoB-N19), and Michael Kracht for JNK3 expression vectors. K.F. is a recipient of a Special Postdoctoral Researchers Fellowship from RIKEN. This work was supported by NIH grants (MH076936 to M.S.; DA017310 to Y.H.), BBSRC (K.C.). M.S. is Investigator of the Howard Hughes Medical Institute.

Received: October 20, 2006
Revised: June 29, 2007
Accepted: September 11, 2007
Published: November 7, 2007

## REFERENCES

Anderson, W.W., and Collingridge, G.L. (2001). The LTP Program: a data acquisition program for on-line analysis of long-term potentiation and other synaptic events. J. Neurosci. Methods *108*, 71–83.

Beique, J.C., and Andrade, R. (2003). PSD-95 regulates synaptic transmission and plasticity in rat cerebral cortex. J. Physiol. *546*, 859–867.

Bingol, B., and Schuman, E.M. (2004). A proteasome-sensitive connection between PSD-95 and GluR1 endocytosis. Neuropharmacology *47*, 755–763.

Brecht, S., Kirchhof, R., Chromik, A., Willesen, M., Nicolaus, T., Raivich, G., Wessig, J., Waetzig, V., Goetz, M., Claussen, M., et al. (2005). Specific pathophysiological functions of JNK isoforms in the brain. Eur. J. Neurosci. *21*, 363–377.

Cheng, D., Hoogenraad, C.C., Rush, J., Ramm, E., Schlager, M.A., Duong, D.M., Xu, P., Rukshan, S., Hanfelt, J., Nakagawa, T., et al. (2006). Relative and absolute quantification of postsynaptic density proteome isolated from rat forebrain and cerebellum. Mol. Cell. Proteomics *5*, 1158–1170.

Coffey, E.T., Smiciene, G., Hongisto, V., Cao, J., Brecht, S., Herdegen, T., and Courtney, M.J. (2002). c-Jun N-terminal protein kinase (JNK) 2/3 is specifically activated by stress, mediating c-Jun activation, in the presence of constitutive JNK1 activity in cerebellar neurons. J. Neurosci. *22*, 4335–4345.

Colledge, M., Snyder, E.M., Crozier, R.A., Soderling, J.A., Jin, Y., Langeberg, L.K., Lu, H., Bear, M.F., and Scott, J.D. (2003). Ubiquitination regulates PSD-95 degradation and AMPA receptor surface expression. Neuron *40*, 595–607.

Craven, S.E., El-Husseini, A.E., and Bredt, D.S. (1999). Synaptic targeting of the postsynaptic density protein PSD-95 mediated by lipid and protein motifs. Neuron *22*, 497–509.

Ehrlich, I., and Malinow, R. (2004). Postsynaptic density 95 controls AMPA receptor incorporation during long-term potentiation and experience-driven synaptic plasticity. J. Neurosci. *24*, 916–927.

El-Husseini, A.E., Schnell, E., Chetkovich, D.M., Nicoll, R.A., and Bredt, D.S. (2000). PSD-95 involvement in maturation of excitatory synapses. Science *290*, 1364–1368.

El-Husseini, A.D., Schnell, E., Dakoji, S., Sweeney, N., Zhou, Q., Prange, O., Gauthier-Campbell, C., Aguilera-Moreno, A., Nicoll, R.A., and Bredt, D.S. (2002). Synaptic strength regulated by palmitate cycling on PSD-95. Cell *108*, 849–863.

Elias, G.M., Funke, L., Stein, V., Grant, S.G., Bredt, D.S., and Nicoll, R.A. (2006). Synapse-specific and developmentally regulated targeting of AMPA receptors by a family of MAGUK scaffolding proteins. Neuron *52*, 307–320.

Futai, K., Kim, M.J., Hashikawa, T., Scheiffele, P., Sheng, M., and Hayashi, Y. (2007). Retrograde modulation of presynaptic release probability through signaling mediated by PSD-95-neuroligin. Nat. Neurosci. *10*, 186–195.

Gao, Y., Dickerson, J.B., Guo, F., Zheng, J., and Zheng, Y. (2004). Rational design and characterization of a Rac GTPase-specific small molecule inhibitor. Proc. Natl. Acad. Sci. USA *101*, 7618–7623.

Gardoni, F., Polli, F., Cattabeni, F., and Di Luca, M. (2006). Calcium-calmodulin-dependent protein kinase II phosphorylation modulates PSD-95 binding to NMDA receptors. Eur. J. Neurosci. *24*, 2694–2704.

Hall, A. (2005). Rho GTPases and the control of cell behaviour. Biochem. Soc. Trans. *33*, 891–895.

Jaffe, H., Vinade, L., and Dosemeci, A. (2004). Identification of novel phosphorylation sites on postsynaptic density proteins. Biochem. Biophys. Res. Commun. *321*, 210–218.

Kim, E., and Sheng, M. (2004). PDZ domain proteins of synapses. Nat. Rev. Neurosci. *5*, 771–781.

Lee, H.K., Kameyama, K., Huganir, R.L., and Bear, M.F. (1998). NMDA induces long-term synaptic depression and dephosphorylation of the GluR1 subunit of AMPA receptors in hippocampus. Neuron *21*, 1151–1162.

Morabito, M.A., Sheng, M., and Tsai, L.H. (2004). Cyclin-dependent kinase 5 phosphorylates the N-terminal domain of the postsynaptic density protein PSD-95 in neurons. J. Neurosci. *24*, 865–876.

Morishita, W., Connor, J.H., Xia, H., Quinlan, E.M., Shenolikar, S., and Malenka, R.C. (2001). Regulation of synaptic strength by protein phosphatase 1. Neuron *32*, 1133–1148.

Mulkey, R.M., Endo, S., Shenolikar, S., and Malenka, R.C. (1994). Involvement of a calcineurin/inhibitor-1 phosphatase cascade in hippocampal long-term depression. Nature *369*, 486–488.

Nakagawa, T., Futai, K., Lashuel, H.A., Lo, I., Okamoto, K., Walz, T., Hayashi, Y., and Sheng, M. (2004). Quaternary structure, protein dynamics, and synaptic function of SAP97 controlled by L27 domain interactions. Neuron *44*, 453–467.

Nakayama, A.Y., Harms, M.B., and Luo, L. (2000). Small GTPases Rac and Rho in the maintenance of dendritic spines and branches in hippocampal pyramidal neurons. J. Neurosci. *20*, 5329–5338.

Oh, M.C., Derkach, V.A., Guire, E.S., and Soderling, T.R. (2006). Extrasynaptic membrane trafficking regulated by GluR1 serine 845 phosphorylation primes AMPA receptors for long-term potentiation. J. Biol. Chem. *281*, 752–758.

Otmakhov, N., Khibnik, L., Otmakhova, N., Carpenter, S., Riahi, S., Asrican, B., and Lisman, J. (2004). Forskolin-induced LTP in the CA1 hippocampal region is NMDA receptor dependent. J. Neurophysiol. *91*, 1955–1962.

Scannevin, R.H., and Huganir, R.L. (2000). Postsynaptic organization and regulation of excitatory synapses. Nat. Rev. Neurosci. *1*, 133–141.

Schluter, O.M., Xu, W., and Malenka, R.C. (2006). Alternative N-terminal domains of PSD-95 and SAP97 govern activity-dependent regulation of synaptic AMPA receptor function. Neuron *51*, 99–111.

Schnell, E., Sizemore, M., Karimzadegan, S., Chen, L., Bredt, D.S., and Nicoll, R.A. (2002). Direct interactions between PSD-95 and stargazin control synaptic AMPA receptor number. Proc. Natl. Acad. Sci. USA *99*, 13902–13907.

Stein, V., House, D.R., Bredt, D.S., and Nicoll, R.A. (2003). Postsynaptic density-95 mimics and occludes hippocampal long-term potentiation and enhances long-term depression. J. Neurosci. *23*, 5503–5506.

Tashiro, A., Minden, A., and Yuste, R. (2000). Regulation of dendritic spine morphology by the rho family of small GTPases: antagonistic roles of Rac and Rho. Cereb. Cortex *10*, 927–938.

Trinidad, J.C., Specht, C.G., Thalhammer, A., Schoepfer, R., and Burlingame, A.L. (2006). Comprehensive identification of phosphorylation sites in postsynaptic density preparations. Mol. Cell. Proteomics *5*, 914–922.

Turrigiano, G.G., and Nelson, S.B. (2004). Homeostatic plasticity in the developing nervous system. Nat. Rev. Neurosci. *5*, 97–107.

Weston, C.R., and Davis, R.J. (2002). The JNK signal transduction pathway. Curr. Opin. Genet. Dev. *12*, 14–21.

Zhu, J.J., Qin, Y., Zhao, M., Van Aelst, L., and Malinow, R. (2002). Ras and Rap control AMPA receptor trafficking during synaptic plasticity. Cell *110*, 443–455.